Impurity-Pinned Solitons in the Two-Dimensional Antiferromagnet Detected by Electron Paramagnetic Resonance

K. Subbaraman, C. E. Zaspel, and John E. Drumheller
Department of Physics, Montana State University, Bozeman, Montana 59717
(Received 25 July 1997)

It is shown that the introduction of a very small amount of nonmagnetic impurities into the magnetic sites of a classical two-dimensional antiferromagnet creates a new type of static (impurity-pinned) soliton that affects the Arrhenius, $\exp(-E/T)$, temperature-dependent electron paramagnetic resonance linewidth by drastically changing the parameter E. Data just above the transition temperature for $(C_3H_7NH_3)_2M_xMn_{1-x}Cl_4$ confirm the existence of these impurity-pinned solitons. [S0031-9007(98)05498-2]

PACS numbers: 75.10.Hk, 75.40.Gb, 76.30.Fc

Two-dimensional magnetic systems support interesting nonlinear excitations including solitons and vortices. For the two-dimensional (2D) isotropic ferromagnetic Belavin and Polyakov [1] obtained these solitonlike solutions (BP solitons) from topological considerations. The energy of this excitation is found to be independent of the soliton size resulting from scale invariance of the continuum Heisenberg Hamiltonian. The significance of these excitations was recognized early in connection with the critical properties of 2D magnets. For example, in [1] it was shown that the existence of large localized excitations will cause the correlation length to remain finite at any nonzero temperature as expected from the Mermin-Wagner theorem [2].

Recently we have shown [3,4] that BP solitons dominate the thermodynamics in the fluctuation region immediately above the Néel temperature of a large class of nearly classical 2D antiferromagnets. Experimentally this is observed as an Arrhenius behavior of the temperature-dependent electron paramagnetic resonance (EPR) linewidth in layered manganese systems which was first predicted by Waldner [5,6]. In [3,4] the EPR linewidth was calculated from the dynamic spin correlation function with the time dependence from the soliton-magnon interaction; moveover, it was shown that the calculated linewidth matched the observed Arrhenius behavior.

In this Letter we show that a new type of soliton pinned to a nonmagnetic impurity will form, and this pinned soliton has a lower energy than a large pinned soliton with a corresponding larger density in the lattice. This lowering of energy for the impurity solitons occurs simply because of elimination of exchange bonds at the impurity, which is a significant effect in the small and a negligible effect in the large impurity solitons. Because of this energy difference, the smaller pinned soliton will dominate the BP soliton in the fluctuation region. In order to relate these small impurity-pinned solitons to experimental data, we first obtain the temperature-dependent EPR linewidth resulting from these structures as a function of impurity concentration. This calculation shows that there will be large changes in the temperature dependence of the EPR linewidth as the impurity concentration is varied in a small (less than 1%) range. Finally, this effect is observed by EPR measurements on manganese compounds with nonmagnetic impurities where the calculated impurity dependence is indeed observed.

We begin with the form of the soliton obtained from the continuum Lagrangian [7] for the classical 2D antiferromagnet with the sublattice magnetization expressed in a spherical coordinate system $l = (\sin\theta\sin\varphi, \sin\theta\sin\varphi, \cos\theta)$, and the lattice plane position given in a polar (r, ϕ) coordinate system

$$L = \frac{Js^2}{2}\int\left[\frac{1}{c^2}\,\theta_t^2 - (\nabla\theta)^2 + \sin^2\theta\left(\frac{1}{c^2}\,\varphi_t^2 - (\nabla\varphi)^2\right)\right]d^2x\,, \quad (1)$$

where c is the magnon velocity and Js^2 is the exchange interaction between nearest neighbors in the ground state. The Belavin-Polyakov excitation [1] is given by $\varphi = \phi$ and $\theta(r) = 2\tan^{-1}(r_0/r)$ where the soliton size r_0 is arbitrary from scale invariance of the Lagrangian. Next, the energy of the soliton is obtained by substitution of the BP form into the Lagrangian resulting in

$$E(r_0) = E_s r_0^2/(r_0^2 + r_c^2)\,, \quad (2)$$

where $E_s = 4\pi Js^2$, and r_c is the lower limit of the integral in Eq. (1). This will be determined when we later consider how the discrete nature of the lattice surrounding the impurity will affect the energy expression. In the following, all length parameters are expressed in units of the lattice constant. For large solitons we notice that r_0 is large compared to other lengths with the result that the energy is independent of r_0, and the sublattice magnetization polar angle at the origin is given by $\theta(0) = \pi$. Furthermore, if $\theta(0) = \pi$, then the entire spin space sphere is mapped onto the lattice plane implying that this is a topological soliton. For small solitons with a corresponding small r_0, the minimum r is the order of one resulting in a nonzero polar angle for the spins at the soliton center. In this case part of the spin space sphere around $\theta = \pi$ is not included in the mapping

which results in a vortexlike singularity at the center. Therefore, the energy and structure in this region must be determined on the discrete lattice rather than in the continuum approximation.

To calculate the impurity-pinned soliton energy and its contribution to the EPR linewidth, we will divide the soliton into two regions consisting of the discrete core and the surrounding continuum region. From Eq. (2) it is seen that the continuum part of the energy will decrease as r_0 becomes smaller, but an increase in the core energy results in the total energy still approximately independent of r_0. However, if there is a nonmagnetic impurity at the soliton center, the exchange interactions here are removed which results in a lower core energy and this is much more pronounced for the smaller solitons (small r_0) than for the larger soliton (large r_0). These impurity-pinned solitons (referred to as I solitons) will be shown to have a larger Boltzmann factor than the topological solitons (referred to as P solitons) found in the pure crystal, and because of their larger Boltzmann factor they dominate the thermodynamics.

In the calculation of the EPR linewidth from the I-type solitons it is first necessary to obtain an expression for their energy similar to Eq. (2) so that thermal averages over the soliton size can be obtained. This is done using a simple technique first developed by Wysin [8] to study vortex stability, and later extended by our group [9] to include nonmagnetic impurities. In this technique the energy is calculated using the discrete Heisenberg Hamiltonian applied to a small core

$$H = J \sum_{i,j} \vec{S}_i \cdot \vec{S}_j \,, \tag{3}$$

where the sum is over nearest neighbors. Figure 1 shows this core with lattice sites indicated by circles, the projection of the spins onto the lattice plane indicated by the arrows, and the exchange interactions between nearest neighbor spins indicated by bonds. Also shown is the central impurity and the missing exchange interactions around the impurity. As was done in [8,9] the core energy in terms of an arbitrary polar spin angle for cores up to radii of $r = 4\sqrt{2}$, lattice constants have been calculated. The energy is determined by assuming a form for $\theta(r)$ which is given by the BP radial dependence of the polar angle. We have also found the polar angle of the discrete spins by numerical solution of the set of nonlinear equations resulting from minimization of the core energy. Either form will result in essentially the same core energy. Next the core energy is added to the continuum contribution given by Eq. (2) to obtain the soliton energy as a function of r_0. This was done for successively larger cores until the total energy becomes independent of the core radius ensuring that the continuum approximation will be valid at the core edge. The soliton energy as a function of r_0 obtained in this way is shown in Fig. 2 for both the P and I solitons. Here the energy decrease of the I soliton is clearly seen as r_0 decreases. In order

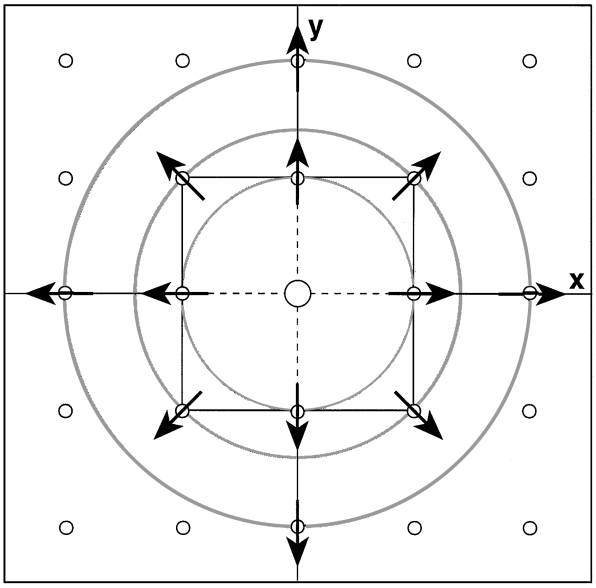

FIG. 1. The smallest core from which the energy is calculated with the impurity ion at the core center. Arrows represent spin projections onto the lattice plane, and the exchange interactions are represented by solid lines.

to calculate thermal averages, the value for the parameter r_c in Eq. (2) is required. This is determined by fitting Eq. (2) to the curves in Fig. 2 giving $r_c = 0.23$ for the P and $r_c = 1.01$ for the I soliton. This expression for the energy is now valid over the whole soliton (core and continuum region). Using these parameters in Eq. (2) will result in different energies for the P and I solitons giving different temperature-dependent EPR linewidths.

Following the method used in [3,4] the EPR linewidth is calculated from the time integral

$$\Delta H \approx \frac{T}{\chi_\perp} \sum_Q A_Q \, \mathrm{Re} \int_0^\infty e^{i\omega_0 t} |\langle S_Q^x(t) S_{-Q}^x(0)\rangle|^2 dt \,, \tag{4}$$

where A_Q is related to the Fourier coefficient of the dipolar interaction and ω_0 is the resonance frequency. The time-dependent spin correlation function is obtained after

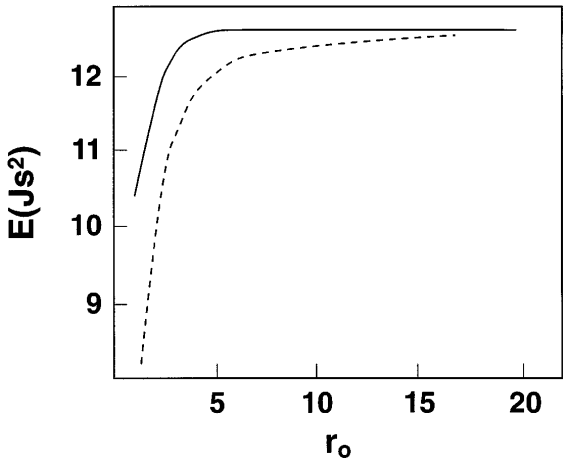

FIG. 2. P-type soliton (solid curve) and I-type soliton (dashed curve) energies versus r_0.

the following simplifying assumptions. First we assume that the magnetization at any point in the lattice is from solitons located at sites $\vec{R}_\alpha$ with $S^x(\vec{r}_i, t) = \sum_\alpha S^x(\vec{r}_i - \vec{R}_\alpha, t)$; this was used to obtain the spin correlation functions [10] from vortices in 2D magnets. The time dependence is assumed to result from the soliton-magnon interaction [11,12] with the magnon scattering from the outer region of the soliton, which will be in the continuum region of the soliton. The change in the soliton structure is assumed to be $\theta(r, t) = \theta_0(r) - \xi(r) \sin\theta_0(r) \cos\omega t$ and $\varphi(r, \phi, t) = \phi + \xi(r) \sin\omega t$ where θ_0 is the static soliton polar angle, and the magnon frequency is $\omega = c|q| - iDq^2/2$ for the antiferromagnet with spin diffusion as the relaxation mechanism. Parameters in the magnon dispersion region for the 2D antiferromagnet [13] are $D = R\sqrt{T/\chi_\perp}$, $c = Js\sqrt{8}$, $\chi_\perp = 1/8J$ and R is the correlation length. The function

$$\xi(r) = 2\omega r_0^2/c\pi^2 r^2 \tag{5}$$

was determined in [3,4] from the perturbed Lagrangian, and it is used to find the static and dynamic contributions to the soliton structure factor. Using these expressions, the time integral in Eq. (4) is done to obtain an expression for the EPR linewidth similar to that in [3,4], but including extra terms resulting from the nonmagnetic impurities. The result is

$$\Delta H \approx R \ln R \sqrt{\frac{T}{\chi_\perp}} \int_{1/R}^{1} \left\{ n_P \langle r_0^2 \rangle_P \left\langle r_0^4 \ln\left(\frac{R}{r_0}\right)\right\rangle_P + n_I \langle r_0^2 \rangle_I \left\langle r_0^4 \ln\left(\frac{R}{r_0}\right)\right\rangle_I + 4\pi^2 n_I n_P \langle r_0^2 \rangle_I \left\langle r_0^4 \ln\left(\frac{R}{r_0}\right)\right\rangle_P \right\} \left\langle \frac{\omega}{c} \right\rangle \frac{dQ}{Q}, \tag{6}$$

where n is the soliton density of either soliton type, and the angular brackets indicate a thermal average over r_0. The subscripts P and I refer to the topological and impurity-centered solitons, respectively.

Next the individual factors in Eq. (6) are evaluated in terms of the temperature and correlation length. If both P and I solitons are present, then the soliton density is the sum of the individual soliton densities $n \approx n_P + n_I$, which results in $n_P = 1/R^2 - n_I$. Finally, n_I is related to the impurity density ρ by $n_I = \rho(1 - P)$ where P is the probability of finding a P soliton at an impurity, which is obtained from the energies of both soliton types. Thermal averages can next be performed for both soliton types using the energy $E(r_0)$ for the P and I solitons. For the P soliton we obtain

$$\langle r_0^2 \rangle_P \approx R/2, \tag{7a}$$

$$\langle r_0^4 \ln(R/r_0) \rangle \approx \tfrac{1}{6} R^2 \ln R. \tag{7b}$$

The calculation of these quantities for the I soliton is somewhat more complicated because of the lower energies at small values of r_0; for these we obtain

$$\langle r_0^2 \rangle_I \approx \left(\frac{2(r_c'^2 + r_c^2)^3}{\sigma} + R\alpha(\sigma + R) \right) \Big/ (\sigma + \alpha R), \tag{8a}$$

$$\left\langle r_0^4 \ln\left(\frac{R}{r_0}\right)\right\rangle_I \approx [R^2\alpha(2R + \sigma)] \ln R/[6(\sigma + \alpha R)], \tag{8b}$$

where $\sigma = E_s r_c^2/T$, and $\alpha = \exp(\sigma/R - \sigma/(r_c'^2 + r_c^2))$. In these expressions r_c' is the lower limit of r_0 when the average over this parameter is done, and r_c is the parameter in the energy expression, which depends on the soliton type. The lower limit of r_0 is estimated by consideration of the quantum nature of the spins. This implies that for the $S = 5/2$ manganese ion, the smallest excitation will have $S_z = 1/2$, $S_z = 3/2$, and $S_z = 5/2$ on the first three concentric circles in Fig. 1. By approximating this structure to the BP form we obtain $r_c' \approx 1$. When these are combined, the temperature-dependent linewidth is determined to be

$$\Delta H \approx T^{5/2} (R \ln R)^2 \left[[1 - \rho(1 - P)R^2] \left(1 + \frac{8\pi^2(1 - P)y}{\sigma + \alpha R}\right) + \frac{2\rho\alpha R(1 - P)(2R + \alpha)y}{(\sigma + \alpha R)^2} \right], \tag{9}$$

with $y = 2(r_c'^2 + r_0^2)^2/\sigma^2 + R\alpha(\sigma + R)$.

Experimental EPR data were obtained for the nearly 2D antiferromagnet [14] ($J/k = 9.2$ K), $(C_3H_7NH_3)_2M_xMn_{1-x}Cl_4$. This is a layered structure which has the onset of long range correlations in the layer immediately above the Néel temperature ($T_N = 39.2$ K); furthermore, the spin of the Mn ion ($S = 5/2$) ensures that this compound is well approximated by the classical Lagrangian. For nonmagnetic doping ions M, we used Mg and Cd grown from a solution with impurity concentrations mostly below 1%. The temperature dependence of the EPR linewidth exhibits a linear region from room temperature down to about 60 K; slightly below this temperature and T_N the Arrhenius behavior is observed. It is in this fluctuation region where the effect of impurity solitons can be observed by measuring the linewidth versus temperature for different impurity concentrations. In order to better see this behavior we have plotted $\ln(\Delta H(T)/\Delta H_{RT})$ versus T_N/T in Fig. 3 showing how the slope decreases dramatically as the Cd impurity concentration increases. Here ΔH_{RT} is the room temperature linewidth (21 G) which is independent of the impurity concentration at these low levels. These data are for the magnesium doped compounds, but cadmium

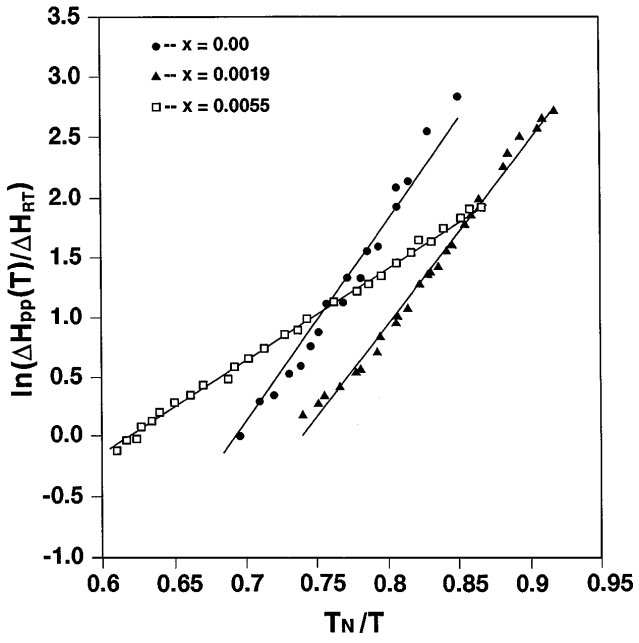

FIG. 3. $\ln[\Delta H/\Delta H(\infty)]$ versus T_N/T for different Cd concentrations.

also shows this behavior. Another interesting impurity effect seen here is noticed in the crossing of the lower and higher concentration curves. This is interpreted to be the result of the soliton size being proportional to the correlation length as assumed in [1]. Since the I solitons are smaller than the P solitons, they can form at a slightly higher temperature when the correlation length is shorter resulting in the Arrhenius behavior beginning at a higher temperature.

Finally, these data are compared with the concentration-dependent linewidth calculated from Eq. (9). To do this we have plotted experimental values of $\ln\Delta H$ versus T_N/T for different impurity concentrations, and the slope of this curve is referred to as the Arrhenius excitation energy E. Some deviation from the Arrhenius form is seen in Eq. (9), but as seen from [3,4] this deviation is negligible compared to the experimental uncertainty.

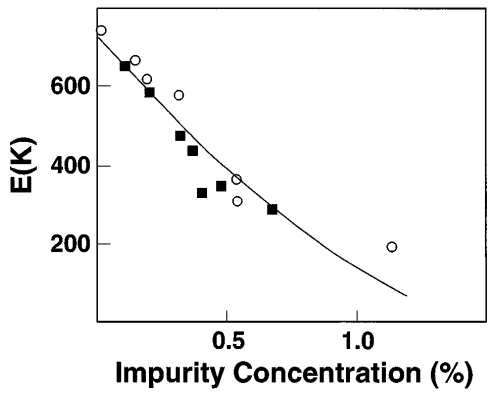

FIG. 4. Excitation energy versus ρ. The circles represent Cd data and the squares represent Mg data. The curve is the theoretical dependence.

Similarly, the deviation from Arrhenius behavior is also negligible for the small impurity concentrations. Next the derivative $d\ln\Delta H/d(T_N/T)$ is numerically calculated using Eq. (5) together with Takahashi's [15] expression for the correlation length

$$R = (8e^{\pi/2}\sqrt{2})^{-1}\exp(E_s/2T), \qquad (10)$$

to obtain the calculated Arrhenius excitation energy. Figure 4 shows the calculated value of E versus concentration and the experimental data for the cadmium and magnesium-doped compounds. It is noticed that both impurities exhibit the same general trend.

Finally, since the excitation energy obtained from the slopes of the graphs will be sensitive to changes in T_N, it is necessary to determine whether the ordering temperature would be affected by these small impurity concentration levels. To check this we have made ac susceptibility measurements (10 Hz–100 kHz) for the diluted compounds. To within experimental uncertainty (± 0.1 K) no change in T_N was observed.

In conclusion, we have detected a small, pinned soliton that tends to form at a nonmagnetic impurity in the layered antiferromagnet. Since solitons are the dominant contribution to the temperature-dependent EPR linewidth, the effect of these pinned solitons is seen as a large change in this dependence when a very small concentration of nonmagnetic impurity is in the crystal.

We acknowledge support from the National Science Foundation, for Grant No. DMR-93109067.

[1] A. A. Belavin and A. M. Polyakov, Pisma Zh. Eksp. Teor. Fiz. **22**, 503 (1975) [JETP Lett. **22**, 245 (1975)].
[2] N. D. Mermin and H. Wagner, Phys. Rev. Lett. **17**, 1133 (1966).
[3] C. E. Zaspel, T. E. Grigereit, and J. E. Drumheller, Phys. Rev. Lett. **74**, 4539 (1995).
[4] C. E. Zaspel and J. E. Drumheller, Int. J. Mod. Phys. B **10**, 3648 (1996).
[5] F. Waldner, J. Magn. Magn. Mater. **31–34**, 1203 (1983).
[6] F. Waldner, J. Magn. Magn. Mater. **104–107**, 793 (1992).
[7] B. A. Ivanov and D. D. Sheka, Phys. Rev. Lett. **72**, 404 (1994).
[8] G. M. Wysin, Phys. Rev. B **49**, 8780 (1994).
[9] C. E. Zaspel, C. M. McKennan, and S. R. Snaric, Phys. Rev. B **53**, 11 317 (1996).
[10] F. G. Mertens, A. R. Bishop, G. M. Wysin, and C. Kawabata, Phys. Rev. B **39**, 591 (1989).
[11] E. Allroth and H. J. Mikeska, Z. Phys. B **43**, 209 (1981).
[12] B. V. Costa, M. E. Gouvea, and A. S. T. Pires, Phys. Lett. A **165**, 179 (1992).
[13] S. Chakravarty, B. I. Halperin, and D. R. Nelson, Phys. Rev. B **39**, 2344 (1989).
[14] H. A. Groenendijk, A. J. Van Duyneveldt, and R. D. Willett, Physica (Amsterdam) **98B**, 53 (1979).
[15] M. Takahashi, Phys. Rev. B **40**, 2494 (1989).